

# CrystEngComm

Accepted Manuscript



This is an *Accepted Manuscript*, which has been through the Royal Society of Chemistry peer review process and has been accepted for publication.

*Accepted Manuscripts* are published online shortly after acceptance, before technical editing, formatting and proof reading. Using this free service, authors can make their results available to the community, in citable form, before we publish the edited article. We will replace this *Accepted Manuscript* with the edited and formatted *Advance Article* as soon as it is available.

You can find more information about *Accepted Manuscripts* in the [Information for Authors](#).

Please note that technical editing may introduce minor changes to the text and/or graphics, which may alter content. The journal's standard [Terms & Conditions](#) and the [Ethical guidelines](#) still apply. In no event shall the Royal Society of Chemistry be held responsible for any errors or omissions in this *Accepted Manuscript* or any consequences arising from the use of any information it contains.



Journal Name

ARTICLE

## Fluorescent and photochromic properties of a series of new Zn(II)/Cd(II) coordination compounds with a flexible semi-rigid tetrazole-viologen derivative

Yu Xiao,<sup>ab</sup> Shuai-Hua Wang,<sup>\*a</sup> Ya-Ping Zhao,<sup>ab</sup> Fa-Kun Zheng,<sup>\*a</sup> and Guo-Cong Guo<sup>a</sup>

Received 00th January 20xx,  
Accepted 00th January 20xx

DOI: 10.1039/x0xx00000x

www.rsc.org/

Photoluminescence coordination compounds have appealing applications in light-emitting and photoactive materials, while there exist some difficulties in the tuning and domination of luminescence by changing the structures. In this work, the diverse luminescence was realized by rational design and controllable construction of a series of Zn(II)/Cd(II) coordination compounds from an isolated binuclear moiety, 1D zigzag chain, 1D ladder-like chain to a 3D 3,4-connected topology network based on a flexible semi-rigid tetrazole-viologen ligand. Especially, the isolated binuclear compound shows an interesting photochromic molecular system that involves electron transfer from N<sub>3</sub><sup>-</sup> ions and Cl atoms to the tetrazole-viologen ligand, and exhibits fluorescence and second-order nonlinear optical property variation upon ultraviolet light irradiation.

### Introduction

Photoluminescence coordination compounds (PLCCs) materials have attracted extensive attention due to their intriguing structures and ever-expanding applications in chemical sensing, lasers, light-emitting devices, biomedical imaging and so on.<sup>1</sup> Compared with conventional inorganic and organic luminescence materials, PLCCs have shown important advantages owing to their rich luminescent emitting centers including ligand-centered, metal-centered, ligand-metal charge transfer and guest molecules.<sup>2</sup> In addition to the composition, the diversities of crystal structure also have great influence on the luminescence properties of coordination compounds.<sup>3</sup> However, it is still difficult to realize the tuning and domination of luminescence by changing the structures. From the perspective of crystal engineering, the semi-rigid organic linkers tend to form various structures in different coordination environments, which may provide directional construction in the crystal self-assembly process of PLCCs.<sup>4</sup> Taking into account functional units, tetrazole groups can provide aromatic nature and multiple coordination modes, which have been used to construct various optical coordination compounds, including optoelectronic devices and photosensitive materials.<sup>5</sup> Therefore, we innovatively design a

flexible semi-rigid tetrazole-viologen ligand, wherein the tetrazole groups can be generated by in-situ [2 + 3] cycloaddition reaction of the cyano precursor and azide (Scheme 1, N-(tetrazolmethyl)-4,4'-bipyridinium regarded as tzmb). Notably, an alkyl -CH<sub>2</sub>- spacer, linking the tetrazole and 4,4'-bipyridinium group in the tzmb ligand, is rotationally free to some extent with different relative orientations to meet the requirements for constructing coordination compounds bearing diverse architectures and functions. Finally, four new coordination compounds of [ZnCl(N<sub>3</sub>)(tzmb)]<sub>2</sub>·H<sub>2</sub>O (**1**), [ZnCl(N<sub>3</sub>)(tzmb)]<sub>n</sub> (**2**), [Zn<sub>2</sub>Cl<sub>3</sub>(OH)(tzmb)]<sub>n</sub> (**3**) and [Cd<sub>2</sub>(N<sub>3</sub>)<sub>2</sub>(C<sub>2</sub>O<sub>4</sub>)(tzmb)<sub>2</sub>]<sub>n</sub> (**4**) were successfully achieved through one-step reactions. The structural analyses and the relationship between the structure and luminescence of these compounds have been discussed. Moreover, compound **1** displays photochromic characteristic, as well as fluorescence and second-order nonlinear optical (NLO) response diminishment accompanying with its color change from pale yellow to olive green, wherein radicals generated among the electron transfer process have been proved by experimental and theoretical results. To the best of our knowledge, this is the first example of tetrazole-viologen-based photochromic coordination compound and the extension of our previous work on the viologen-based photochromic compounds.<sup>6</sup> Compared with the carboxylate-viologen compounds, the introducing of tetrazole group provides more profuse electron donor in the charge transfer process and interesting luminescence, nonlinear optical, electrochemical performances for the products.<sup>7</sup>

*a* State Key Laboratory of Structural Chemistry, Fujian Institute of Research on the Structure of Matter, Chinese Academy of Sciences, Fuzhou, Fujian, 350002, PR China. E-mail: zfk@fjirsm.ac.cn; Fax: +86 591 6317 3068; Tel: +86 591 63173889

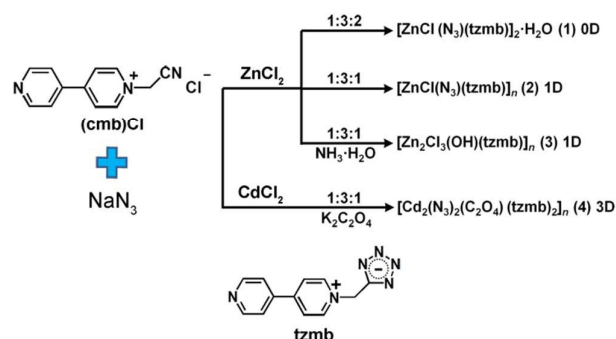
*b* University of Chinese Academy of Sciences, Beijing 100039, PR China

† Electronic Supplementary Information (ESI) available: Additional tables of structural data, IR, PXRD patterns, TGA and luminescence decay curves, excitation and emission spectra. CCDC 1451442 and 1029757-1029759.

For ESI and crystallographic data in CIF or other electronic format. See DOI: 10.1039/x0xx00000x

### Experimental section

#### Materials and instruments



**Scheme 1.** The synthetic route of 1–4. The reactant molar ratios (cmb)Cl/NaN<sub>3</sub>/ZnCl<sub>2</sub>(CdCl<sub>2</sub>) are 1:3:2, 1:3:1, 1:3:1, 1:3:1 for 1–4, respectively.

All reagents purchased commercially were used without further purification. Free ligand (Htzmb)Cl was prepared by treating compound 1 with 1 N hydrochloric acid according to our previously described procedure.<sup>8</sup> Powdered X-ray diffraction (PXRD) patterns were collected on a Rigaku Miniflex II diffractometer using Cu-K $\alpha$  radiation ( $\lambda = 1.540598 \text{ \AA}$ ) at 40 kV and 40 mA in the range of  $5 \leq 2\theta \leq 60^\circ$ . The simulated PXRD patterns were derived from the Mercury Version 1.4 software (<http://www.ccdc.cam.ac.uk/products/mercury/>).

The elemental analyses were performed on an Elementar Vario EL III microanalyzer. The FT-IR spectra were obtained on a Perkin-Elmer Spectrum using KBr disks in the range 4000–400 cm<sup>-1</sup>. Thermogravimetric analysis (TGA) experiments were done on a NETZSCH STA 449C Jupiter thermogravimetric analyzer in N<sub>2</sub> with the sample heated in an Al<sub>2</sub>O<sub>3</sub> crucible at a heating rate of 10 K min<sup>-1</sup>. The determination of photoluminescence (PL) and lifetime was conducted on a double excitation monochromator Edinburgh FL920 fluorescence spectrometer equipped with a R928 PMT detector.

### Synthesis of compounds

**Synthesis of N-(cyanomethyl)-4,4'-bipyridinium chloride.** A mixture of chloroacetonitrile (2.27 g, 0.03 mol) and 4,4'-bipyridine (4.68 g, 0.03 mol) in 25 mL DMF was stirred for 2h, and then heated to 80 °C. The stirring was continued and kept to this temperature for one day, and then the brown precipitates were filtered. The compound N-(cyanomethyl)-4,4'-bipyridinium chloride ((cmb)Cl) was obtained with 53% yield. NMR analysis for (cmb)Cl, <sup>1</sup>H NMR (400 MHz, D<sub>2</sub>O):  $\delta$  9.20 (d, J = 6.3 Hz, 2H), 8.88 (d, J = 6.5 Hz, 2H), 8.57 (d, J = 6.8 Hz, 2H), 8.41 (d, J = 6.7, 2H), 5.52 (d, J = 6.1 Hz, 2H). Anal. Calcd for C<sub>12</sub>H<sub>10</sub>N<sub>3</sub>Cl: C, 62.21; H, 4.35; N, 18.14 %. Found: C, 62.93; H, 4.61; N, 18.56%.

**Synthesis of [ZnCl(N<sub>3</sub>)(tzmb)]<sub>2</sub>·H<sub>2</sub>O (1).** A mixture of ZnCl<sub>2</sub> (64.0 mg, 0.4 mmol), (cmb)Cl (51.0mg, 0.2 mmol), NaN<sub>3</sub> (41.0 mg, 0.6 mmol) and H<sub>2</sub>O (8 mL) was placed in a 25 mL Teflon-lined stainless steel vessel. The mixture was sealed and heated at 140 °C in two hours and kept to this temperature for two days and cooled to room temperature at a rate of 5 °C/h. Block crystals for 1 were obtained with a yield of 56% (based on Zn). Anal. Calcd for C<sub>24</sub>H<sub>22</sub>N<sub>18</sub>OCl<sub>2</sub>Zn<sub>2</sub> (1): C, 36.94; H, 2.84; N, 32.31%. Found: C, 36.63; H, 2.42; N, 32.73%. IR (KBr pellet, cm<sup>-1</sup>) for 1: 3402m, 3044w, 2078vs, 1614s, 1544m, 1466m, 1424s,

1347m, 1283w, 1164m, 1073m, 869w, 805s, 749m, 706m, 503m.

**Synthesis of [ZnCl(N<sub>3</sub>)(tzmb)]<sub>n</sub> (2).** A mixture of ZnCl<sub>2</sub> (68.3 mg, 0.5 mmol), (cmb)Cl (115.8mg, 0.5 mmol), NaN<sub>3</sub> (97.5 mg, 1.5 mmol) and H<sub>2</sub>O (10 mL) was placed in a 25 mL Teflon-lined stainless steel vessel. The mixture was sealed and heated at 140 °C in two hours and kept to this temperature for two days and cooled to room temperature at a rate of 5 °C/h. Block crystals for 2 were obtained with a yield of 32% (based on Zn). Anal. Calcd for C<sub>12</sub>H<sub>10</sub>N<sub>9</sub>ClZn (2): C, 37.82; H, 2.64; N, 33.08%. Found: C, 37.67; H, 2.83; N, 33.31%. IR (KBr pellet, cm<sup>-1</sup>) for 2: 3425m, 3040m, 2080vs, 1642s, 1545m, 1472w, 1409s, 1345m, 1288m, 1173s, 864w, 803vs, 732m, 680m, 480w.

**Synthesis of [Zn<sub>2</sub>Cl<sub>3</sub>(OH)(tzmb)]<sub>n</sub> (3).** The same synthetic method as that for 2 was used with additional NH<sub>3</sub>·H<sub>2</sub>O (17.5 mg, 0.5mmol). Yield: 28% (based on Zn). Anal. Calcd for C<sub>12</sub>H<sub>11</sub>N<sub>6</sub>OCl<sub>3</sub>Zn<sub>2</sub> (3): C, 29.27; H, 2.25; N, 17.07%. Found: C, 29.50; H, 2.30; N, 17.16%. IR (KBr pellet, cm<sup>-1</sup>) for 3: 3540vs, 3014s, 2087s, 1956w, 1642vs, 1607vs, 1541s, 1421vs, 1327m, 1231w, 1178s, 1074s, 978s, 829vs, 800vs, 746s, 689w, 541vs, 480s.

**Synthesis of [Cd<sub>2</sub>(N<sub>3</sub>)<sub>2</sub>(C<sub>2</sub>O<sub>4</sub>)(tzmb)]<sub>n</sub> (4).** A mixture of Cd(NO<sub>3</sub>)<sub>2</sub>·4H<sub>2</sub>O (154.3 mg, 0.5 mmol), (cmb)Cl (115.8 mg, 0.5 mmol), NaN<sub>3</sub> (97.5 mg, 1.5 mmol), K<sub>2</sub>C<sub>2</sub>O<sub>4</sub> (55.3 mg, 0.3 mmol) and H<sub>2</sub>O (10 mL) was placed in a 25 mL Teflon-lined stainless steel vessel. The mixture was sealed and heated at 140 °C in two hours and kept to this temperature for two days and cooled to room temperature at a rate of 5 °C/h. Yield: 12% (based on Cd). Anal. Calcd for C<sub>26</sub>H<sub>20</sub>N<sub>18</sub>O<sub>4</sub>Cd<sub>2</sub> (4): C, 35.76; H, 2.31; N, 28.87%. Found: C, 35.35; H, 2.10; N, 28.64%. IR (KBr pellet, cm<sup>-1</sup>) for 4: 3451m, 3040m, 3005m, 2044vs, 1628vs, 1490m, 1416m, 1327s, 1217m, 1153s, 881w, 794m, 741m, 484m.

### Crystal Structure Determination

Single-crystal X-ray diffraction measurements were carried out on a Rigaku Mercury CCD diffractometer, which was equipped with Mo-K $\alpha$  radiation ( $\lambda = 0.71073 \text{ \AA}$ ), using the  $\omega$ -scan technique for collections of the intensity data sets, and corrected for  $L_p$  effects. The primitive structures were solved by the direct method and reduced by CrystalClear software.<sup>9</sup> The subsequent successive difference Fourier syntheses yielded the other non-hydrogen atoms. For compound 1, in this heavy-atom structure as it was not possible to see clear electron-density peaks in difference maps which would correspond with acceptable locations for the H atoms bonded to water oxygen atom O1W, the refinement was completed with no allowance for these water H atoms in the model. The final structures were refined using a full-matrix least-squares refinement on  $F^2$ . All of the calculations were performed by the Siemens SHELXTL version 5 package of crystallographic software<sup>10</sup>. Pertinent crystal data and structural refinement results, and selected bond distances and angles for 1–4 are listed in Table S1.

### Theoretical calculation

The DFT calculation of the [Zn<sub>2</sub>Cl<sub>2</sub>(N<sub>3</sub>)<sub>2</sub>(tzmb)<sub>2</sub>] molecule of 1 in the triplet ground state was performed using the Gaussian 09

program (Revision D.01) based on the 6-31+g(d, p) basis set and B3LYP functional<sup>11</sup>. The structure was not optimized considering the space confinement of structural variation in the crystal. No spin density distribution can be found from the open-shell singlet state.

## Results and discussion

### Syntheses

Synthesis of tetrazole organic compounds by [2 + 3] cycloaddition of an azide to a nitrile is an effective method, and we have synthesized some classes of coordination compounds based on in situ generated tetrazolate derivatives<sup>12</sup>. In this study, we employed the cyano precursor of N-(cyanomethyl)-4,4'-bipyridinium chloride ((cmb)Cl) and azide anions to successfully obtain tetrazole-based 1–4. The experiment results show that the cycloaddition reaction of synthesizing tetrazoles can work under different conditions, such as alkalic environment or existence of other inorganic components. The in-situ hydrothermally synthesized tetrazole groups of the tzmb ligand were confirmed by IR spectra of 1–4 (Fig. S1). With the disappearance of cyano groups in  $\sim 2200\text{ cm}^{-1}$ , the characteristic peaks of tetrazolate group (at ca. 1466 and 1424  $\text{cm}^{-1}$  for 1, ca. 1472 and 1409  $\text{cm}^{-1}$  for 2, ca. 1541 and 1421  $\text{cm}^{-1}$  for 3, ca. 1490 and 1416  $\text{cm}^{-1}$  for 4, respectively) emerged in the IR spectra. The peaks centered at 2078  $\text{cm}^{-1}$  for 1, 2080  $\text{cm}^{-1}$  for 2 and 2044  $\text{cm}^{-1}$  for 4 reveal the existence of azide groups. Thermogravimetric analyses (TGA) curves (Fig. S2) demonstrate that 1 showed a weight loss of 2.8% in the temperature range of 30–135 °C, corresponding to the removal of lattice water molecules (calcd: 2.3%), and the framework began to collapse above 200 °C. Compounds 2, 3 and 4 can be stable high up to 260, 300 and 300 °C respectively, which may be the consequence of no coordinated or lattice water molecules. The experimental PXRD patterns of the bulk products are consistent with the calculated ones based on the single-crystal data, indicating pure phase of 1–4 (Fig. S3).

### Crystal structure and characterization

**[ZnCl(N<sub>3</sub>)(tzmb)]<sub>2</sub>·H<sub>2</sub>O (1)** single-crystal X-ray diffraction analysis shows that compound 1 crystallizes in the acentric space group *Pn* and exhibits an isolated binuclear unit. As shown in Fig. 1, compound 1 is built upon a discrete [ZnCl(N<sub>3</sub>)(tzmb)]<sub>2</sub> molecular unit, where two Zn(II) atoms are doubly bridged by two neutral tzmb ligands. Each Zn(II) atom has a distorted tetrahedron environment with one terminal chloride ion, one terminal azide anion and two nitrogen atoms from two tzmb ligands. The coordination arrangements make the distances between the Cl ions and the N atoms of the viologen ring being 3.408(4) and 3.557(4) Å, respectively, and also offer an opportunity for an inter-ligand charge transfer between the Cl ions and viologen groups (smaller than 3.7 Å). The tzmb ligand shows a  $\mu_2$ - $\kappa$ N11, $\kappa$ N16 bridging mode in 1. The  $\pi$ ··· $\pi$  stacking interactions are among the two adjacent phenyl groups of tzmb ligands with centroid-to-centroid distances of ca. 3.926(8) and 3.772(7) Å, respectively.

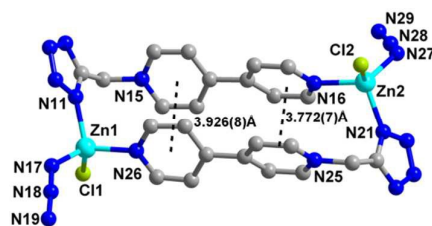


Fig. 1 The isolated binuclear structure of 1. Hydrogen atoms and lattice water molecules are omitted for clarity.

**[ZnCl(N<sub>3</sub>)(tzmb)]<sub>n</sub> (2)** Compound 2 crystallizes in the monoclinic space group *P2<sub>1</sub>/c*. There exist one crystallographically independent Zn(II) atom, one coordinated Cl ion, one terminal azide anion, and one tzmb ligand in an asymmetric unit (Fig. 2a). The Zn1 atom shows a four-coordinated center to form a distorted tetrahedron with Zn–N bond distances in normal range of 2.000(4)–2.033(3) Å, and the Zn1–Cl1 bond distance of 2.209(1) Å. In 1, the tzmb ligand shows a  $\mu_2$ - $\kappa$ N1, $\kappa$ N3 bridging mode to connect Zn atoms, and the pyridine nitrogen atom is not involved in coordination. Two Zn atoms are connected with the tetrazole group giving rise to a 1D zigzag chain, and the 4,4'-bipyridinium group stretches to the two sides of the 1D chain (Fig. 2b). An appealing feature of 2 is the neighboring zigzag chains run in two different directions parallel to the *bc* plane, and face-to-face  $\pi$ ··· $\pi$  interactions are formed with the centroid-to-centroid distance of 3.722(2) Å for antisymmetric 4,4'-bipyridinium groups (Fig. S4), which attributes to dipole-dipole interactions<sup>13</sup>. There exist other  $\pi$ ··· $\pi$  stacking interactions with the centroid-to-centroid distance of 3.932(2) Å, which overlaps stacking along the *a* axis.

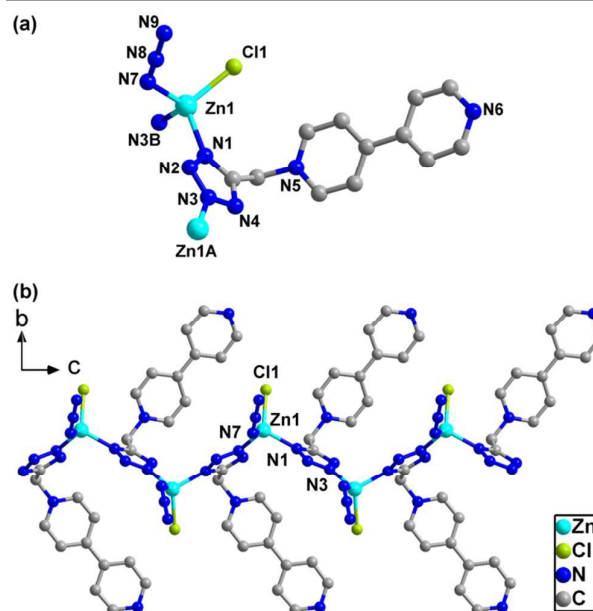


Fig. 2 (a) The coordination environments around the Zn(II) ion and tzmb ligand in 2. Symmetry codes: (A)  $x, 0.5 - y, 0.5 + z$ ; (B)  $x, 0.5 - y, -0.5 + z$ . (b) The 1D zigzag chain of 2 along the *c* axis. Hydrogen atoms are omitted for clarity.

Table 1 Crystal data and structural refinements for compounds 1–4

Complex	1	2	3	4
Empirical formula	C <sub>24</sub> H <sub>22</sub> Cl <sub>2</sub> N <sub>18</sub> OZn <sub>2</sub>	C <sub>12</sub> H <sub>10</sub> N <sub>9</sub> ClZn	C <sub>12</sub> H <sub>11</sub> N <sub>6</sub> OCl <sub>3</sub> Zn <sub>2</sub>	C <sub>26</sub> H <sub>20</sub> N <sub>18</sub> O <sub>4</sub> Cd <sub>2</sub>
<i>M<sub>r</sub></i> (g mol <sup>-1</sup> )	780.23	381.11	492.36	873.40
Crystal system	Monoclinic	Monoclinic	Monoclinic	Monoclinic
Space group	<i>Pn</i>	<i>P2<sub>1</sub>/c</i>	<i>P2<sub>1</sub>/c</i>	<i>P2<sub>1</sub>/c</i>
<i>a</i> (Å)	10.467(3)	7.372(4)	8.026(2)	8.9251(7)
<i>b</i> (Å)	13.587(4)	21.350(11)	16.449(4)	9.9975(8)
<i>c</i> (Å)	11.900(4)	9.953(6)	12.895(3)	16.7168(13)
$\alpha$ (°)	90	90	90	90
$\beta$ (°)	112.036(7) <sup>o</sup>	105.790(9)	102.776(8)	90.338(6)
$\gamma$ (°)	90	90	90	90
<i>V</i> (Å <sup>3</sup> )	1568.8(8)	1507.4(14)	1660.2(7)	1491.6(2)
<i>Z</i>	2	4	4	2
<i>D<sub>c</sub></i> /g cm <sup>-3</sup>	1.652	1.679	1.970	1.945
$\mu$ /mm <sup>-1</sup>	1.753	1.820	3.385	1.496
<i>F</i> (000)	788.0	768.0	976.0	860.0
Reflections collected	11438	9020	10428	10829
Unique Reflections	5303	2725	3077	3303
GOF	1.063	1.043	1.003	1.107
<i>R</i> <sub>1</sub> <sup>a</sup> [ <i>I</i> > 2 $\sigma$ ( <i>I</i> )]	0.0522	0.0376	0.0476	0.0267
<i>wR</i> <sub>2</sub> <sup>b</sup> (all data)	0.1344	0.1021	0.1250	0.0682
Flack	0.121(12)			
CCDC No.	1451442	1029757	1029758	1029759

$$^a R_1 = \sum(F_o - F_c)/\sum F_o; ^b wR_2 = [\sum w(F_o^2 - F_c^2)^2/\sum w(F_o^2)^2]^{1/2}$$

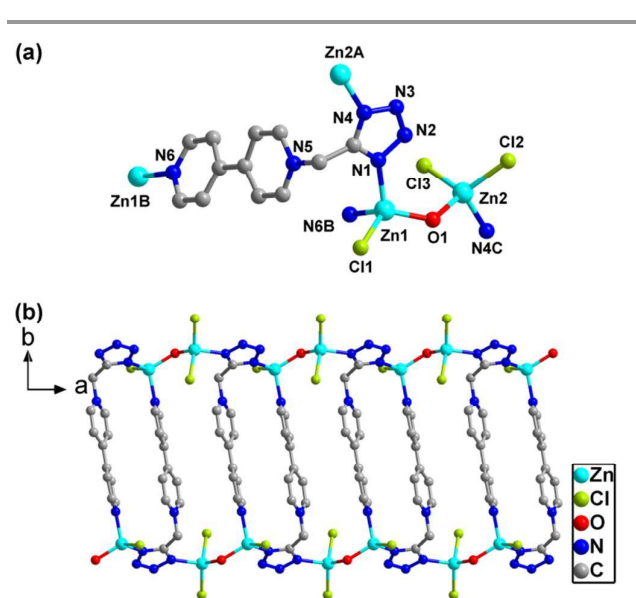


Fig. 3 (a) The coordination environments of **3**. Symmetry codes: (A)  $1 + x, y, z$ ; (B)  $1 - x, 2 - y, 1 - z$ ; (C)  $-1 + x, y, z$ . (b) The 1D ladder-like chain structure of **3** along the *a* axis. Hydrogen atoms are omitted for clarity.

**[Zn<sub>2</sub>Cl<sub>3</sub>(OH)(tzmb)]<sub>n</sub> (3)** Compound **3** crystallizes in the monoclinic space group *P2<sub>1</sub>/c*, and the asymmetric unit contains two crystallographically independent Zn(II) atoms, three coordinated Cl atoms, one OH<sup>-</sup> anion and one tzmb ligand (Fig. 3a). Both the Zn1 and Zn2 centers are four-coordinated with a distorted tetrahedral geometry. The Zn1 atom is surrounded by one Cl atom, one OH<sup>-</sup> anion and two N atoms coming from two different tzmb ligands. The Zn2 atom bonds two Cl atoms, one OH<sup>-</sup> anion and one N atom from tetrazolyl groups. The Zn–N/O bond distances fall in the range of 1.915(3)–2.077(4) Å, and the Zn–Cl bond distances lie in the range of 2.230(2)–2.251(2) Å. The OH<sup>-</sup> anion bridges Zn1 and Zn2 atoms to form a binuclear unit of [Zn<sub>2</sub>Cl<sub>3</sub>(OH)] with the distance of 3.493(1) Å for Zn1…Zn2, and the angle of 129.56(18)<sup>o</sup> for Zn1–O1–Zn2. The structural analysis reveals that the tzmb ligand takes a  $\mu_3$ - $\kappa$ N1, $\kappa$ N4, $\kappa$ N6 bridging mode. Each binuclear unit is connected by the tetrazolate group of tzmb ligand to form a zigzag chain along the *a* axis. Finally, two antiparallel zigzag chains are connected by sharing Zn2–N6 bonds to produce a 1D ladder-like chain (Fig. 3b). These chains stack together in an  $\cdots$ ABAB $\cdots$  fashion along the *c* axis (Fig. S5).

**[Cd<sub>2</sub>(N<sub>3</sub>)<sub>2</sub>(C<sub>2</sub>O<sub>4</sub>)(tzmb)<sub>2</sub>]<sub>n</sub> (4)** In an asymmetric unit of **4**, there are one Cd(II) atom, one terminal azide anion, half a C<sub>2</sub>O<sub>4</sub><sup>2-</sup>

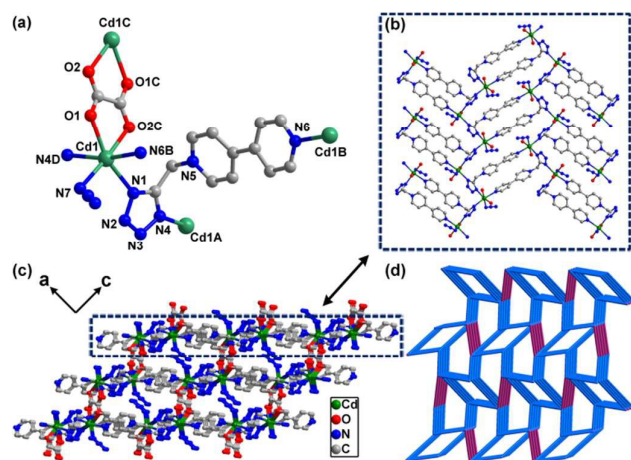


Fig. 4 (a) The coordination environments of **4**. Symmetry codes: (A)  $1-x, -0.5+y, 0.5-z$ ; (B)  $2-x, -y, -z$ ; (C)  $1-x, 1-y, -z$ ; (D)  $1-x, 0.5+y, 0.5-z$ . (b) 2D layer substructure in **4**. (c) 3D network of **4**. (d) Network topology of **4**.

group and one tzmb ligand (Fig. 4a). The  $C_2O_4^{2-}$  anion is united through an inversion center. The Cd(II) atom is six-coordinated by four nitrogen atoms (N1, N4D and N6B atoms from three different tzmb ligand, and N7 atom from one azide anion) and two oxygen atoms (O1 and O2C atoms from carboxylate group) to form a distorted octahedron. The O/N-Cd-O/N angles vary from  $72.49(6)$  to  $175.31(7)^\circ$  and the Cd-O/N distances are in the range of  $2.282(2) - 2.452(2) \text{ \AA}$ , which are all similar to the values found in other reported Cd(II) complexes<sup>14</sup>. It is noteworthy that the tzmb ligand serves as a  $\mu_3$ -bridging linker connecting three Cd(II) ions. Firstly, the Cd(II) ions are bridged by tetrazolyl rings to form a 1D zigzag chain along the *b*-direction with the distance of  $6.7907(4) \text{ \AA}$  for Cd1...Cd1A, and then each chain is alternately interconnected by N6 atoms of 4,4'-bipyridinium groups to form a 2D layer parallel to the *ac* plane (Fig. 4b). The binuclear unit of  $[Cd(N_3)(tzmb)]_2$  is formed, and this layer can also be regarded as coupling of binuclear units by sharing the Cd1–N1 bonds. Finally, neighboring layers are interconnected by  $\mu^2$ - $C_2O_4^{2-}$  group to construct a 3D network of **4** (Fig. 4c). For better insight into intricate polymeric framework, we can use a topological analysis to simplify 3D framework of **4**. Taking the  $C_2O_4^{2-}$  group as a linker bridging two Cd atoms, the Cd atom as a 4-connecting node and one tzmb ligand as a 3-connecting node, the complicated network of **4** can be treated as a two nodal 3,4-connect net  $(4.8^2 \cdot 10^3)(4.8^2)$  (Fig. 4d).

#### Luminescent properties

It is well known that electronically saturated  $d^{10}$  transition metal imposes conformational rigidity to the ligand and prevents energy loss via bond vibration or electron transfer processes, which can yield linker-based highly emissive materials<sup>3a,15</sup>. Therefore, the solid-state excitation and emission spectra for **1–4** and tzmb ligand were investigated at room temperature. The maximum emission peaks of **1–4** are mainly centered at 550, 500, 555 and 565 nm, respectively, and yellow, green, yellow and yellow fluorescences are found by visual observation with optimum excitations of 470, 400,

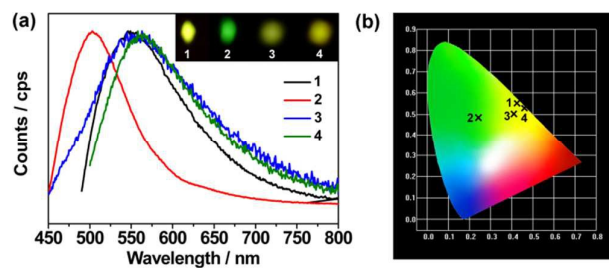


Fig. 5 (a) Normalized fluorescence curves of **1–4** upon 470, 400, 420 and 470 nm excitations. The inset shows relative fluorescence images. (b) CIE chromaticity diagrams of **1–4**.

420 and 470 nm, respectively. Their values of chromaticity coordinates (**1–4**) are (0.43, 0.55), (0.24, 0.48), (0.41, 0.50) and (0.46, 0.53), respectively (Fig. 5a). Compared with the tzmb ligand (maximum emission located at 500 nm with 418 nm excitation) (Fig. S6), luminescent emissions of **1–4** should be attributed to the ligand-centered emission. The values of fluorescent lifetime exhibit 4.09, 21.37, 3.12 and 3.65 ns for **1–4**, respectively (Fig. S7).

As we know that the luminescence characteristic of PLCCs depends on their structures. The size of the metal, the structure of the secondary building units (SBUs) and the orientation of the linkers all affect the emission properties of the material<sup>16</sup>. Compounds **1–4** contain the same linker in different coordination modes and geometries, allowing for a comparative study of their photoluminescence diversity and the  $\pi$ -overlap degree of the organic linkers in the SBU structure. We can find that there is a common dinuclear SBU  $[M_2(tzmb)_2]$  ( $M = Zn$  or Cd) in the structures of compounds **1, 3** and **4**, wherein exist  $\pi \cdots \pi$  stacking interactions between the pyridine rings (Fig. S8). However, such dinuclear SBU is absent in **2**. This is maybe the reason that compounds **1, 3** and **4** display similar emission character, which is different from that of **2**. Compared with the emission wavelength of **2**, the longer emission wavelength of compounds **1, 3** and **4** should be attributed to the increased  $\pi \cdots \pi$  stacking interactions<sup>17</sup>.

#### Photochromism

One of interesting findings was that the crystalline sample of **1** showed a color change from pale yellow to olive green upon continuous irradiation with a 300 W Xe lamp. Meanwhile, the UV/Vis diffuse reflectance spectra generated two new absorption peaks centered at  $\sim 400$  and 604 nm, respectively,

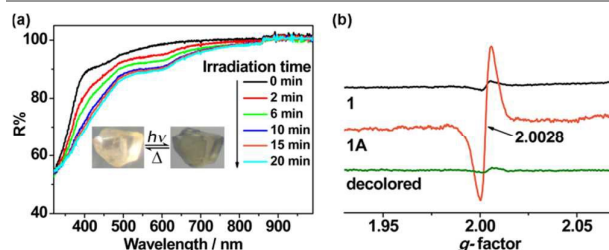


Fig. 6 (a) UV/Vis diffuse reflectance spectral changes of **1** upon ultraviolet light irradiation. (b) ESR spectra of **1**. The small signal around  $g = 2.00$  is for the sample before irradiation, and decolorated sample was caused by unexpected light during sample handling and ESR measurements.

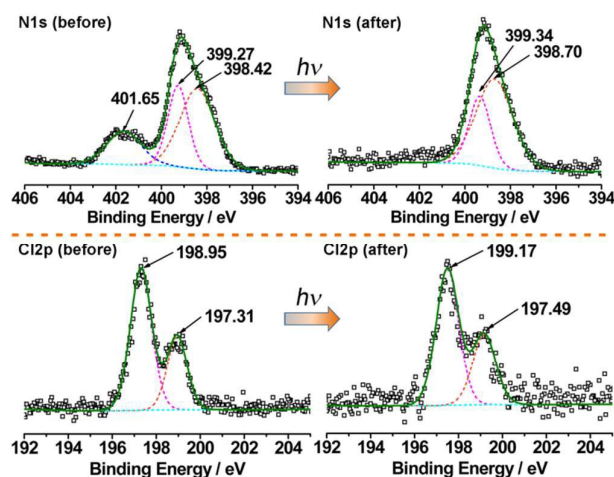


Fig. 7 XPS core-level spectra of **1** before and after irradiation. The blue, pink and orange dashed lines depict the resolved peaks, the sum of which is shown using green solid lines.

which is characteristic of the one-electron reduced species of viologen compounds<sup>18</sup>. The absorption increased with extending the irradiation time and had no further clear variation after 15 mins (Fig. 6a). The photoproduct of **1** (hereafter named as **1A**) can be kept in the dark for several weeks, but easily decolorized after being annealed at 100 °C for 2 h in the air. ESR spectra show that there was no ESR signal before irradiation, but a symmetric single line signals with  $g = 2.0028$  emerged after coloration, which supports that it generated viologen radicals among the electron transfer process (Fig. 6b). Such a radical signal almost disappeared after decoloration, reflecting the reversible nature of photochromism. To elucidate the origin of radicals, a density functional theory (DFT) calculation based on the 6-31+g(d, p) basis set and B3LYP functional was performed. The calculated spin density of the  $[\text{Zn}_2\text{Cl}_2(\text{N}_3)_2(\text{tzmb})_2]$  molecule of **1** in the triplet ground state is shown in Fig. S9. It can be seen that the spins almost distribute in the tzmb ligands,  $\text{N}_3^-$  and  $\text{Cl}^-$  ions. This implies that the tzmb ligand behave as an electron acceptor while the  $\text{N}_3^-$  and  $\text{Cl}^-$  ions as electron donors. X-ray photoelectron spectroscopy (XPS) data of **1** further demonstrate this conclusion. As illustrated in Fig. 7, the N 1s core-level spectrum shows that there are three N components in their structures at the binding energy of  $\sim 398.42$ , 399.27 and 401.65 eV, which can be assigned to the coordinated and uncoordinated N atoms and the positively charged N atoms, respectively, evidenced by the ratio of peak area and the number of elements. After illumination, the positively charged N atom peak disappears and another two N components peaks shift to a higher binding energy (398.70 and 399.34 eV) with the area ratio changing from 5:3 (before irradiation) to 6:3 (after irradiation), suggesting that the positively charged N atom receives electrons and other N components lose electrons. Meanwhile, the Cl 2p core-level spectrum changes obviously after irradiation. Before illumination, the Cl 2p core-level spectrum can be fitted to one pair of spin-orbit-split

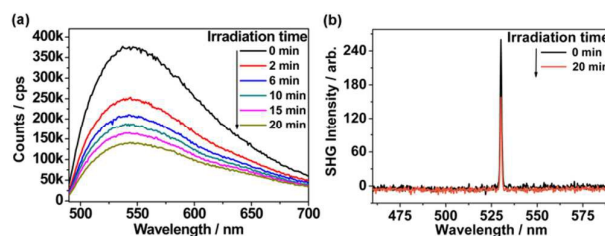


Fig. 8 Fluorescence ( $\lambda_{\text{ex}} = 470 \text{ nm}$ ) (a) and SHG intensity (b) changes of **1** upon ultraviolet light irradiation.

doublets Cl  $2p_{3/2}$  and Cl  $2p_{1/2}$  peaks, lying at  $\sim 197.31$  and 198.95 eV, respectively. After irradiation, the binding energy shifts to the higher positions (197.49 and 199.17 eV), denoting that the  $\text{Cl}^-$  ions lose electrons.

Coupled with the photochromic process, the photoluminescence intensity of **1** shows a gradual decrease with the time of irradiation with a Xe lamp and reaches  $\sim 37\%$  of the starting value after illumination for 20 mins (Fig. 8a). On the other hand, second-harmonic generation (SHG) measurement indicates that the crystalline sample **1** is SHG-active. The most striking feature of **1** is that its SHG response signal becomes smaller after photoinduced coloration, suggesting the potential photo switching of NLO properties. Upon irradiation with a Xe lamp, the SHG intensity of **1** drops approximately 40% of the original value after 20 mins (Fig. 8b), which may arise from the change of molecule polarity during the photoinduced electron transfer process<sup>19</sup>.

## Conclusions

In summary, we have successfully obtained four tetrazole-viologen-based Zn(II)/Cd(II) coordination compounds by designing the in situ generated tzmb ligand, which exhibits strong binding ability with diverse coordination modes by single-bond free rotation of the semi-rigid tzmb ligand. Various structural networks are formed, with an isolated binuclear moiety for **1**, 1D zigzag chain for **2**, 1D ladder-like chain for **3**, and 3D 3,4-connected topology network of **4**. Compounds **1–4** display ligand-centered emissions, and  $\pi\cdots\pi$  stacking interactions have effects on their fluorescence performances. It's mentionable that the crystal of **1** displays photochromic characteristic, and diminishment of the luminescence intensity and SHG response with the color change from pale yellow to olive green upon ultraviolet light irradiation. In short, the semi-rigid tzmb ligand, regarded as a flexible linker, presents potential applications in constructing multifunction materials.

## Acknowledgements

This work was financially supported by 973 Program (2011CBA00505) and National Nature Science Foundation of China (21371170)

## Notes and references

- 1 (a) J. Rocha, L. D. Carlos, F. A. Almeida Paz and D. Ananias, *Chem. Soc. Rev.*, 2011, **40**, 926; (b) Z. Hu, B. J. Deibert and J. Li, *Chem. Soc. Rev.*, 2014, **43**, 5815; (c) X. Yan, T. R. Cook, P. Wang, F. Huang and P. J. Stang, *Nat. Chem.*, 2015, **7**, 342; (d) H. Xu, J. Wang, Y. Wei, G. Xie, Q. Xue, Z. Deng and W. Huang, *J. Mater. Chem. C*, 2015, **3**, 1893; (e) Q. An, J. Liu, M. Yu, J. Wan, D. Li, C. Wang, C. Chen and J. Guo, *Small*, 2015, **11**, 5675.
- 2 (a) Y. Cui, Y. Yue, G. Qian and B. Chen, *Chem. Rev.*, 2012, **112**, 1126; (b) J. Heine and K. Mueller-Buschbaum, *Chem. Soc. Rev.*, 2013, **42**, 9232.
- 3 (a) M. D. Allendorf, C. A. Bauer, R. K. Bhakta and R. J. T. Houk, *Chem. Soc. Rev.*, 2009, **38**, 1330; (b) M. Knorr, A. Khatyr, A. D. Aleo, A. El Yaagoubi, C. Strohmman, M. M. Kubicki, Y. Rousselin, S. M. Aly, D. Fortin, A. Lapprand and P. D. Harvey, *Cryst. Growth & Des.*, 2014, **14**, 5373; (c) M. D. Allendorf and V. Stavila, *Crystengcomm*, 2015, **17**, 229; (d) S. Gao, Q. Fan, X. M. Wang, L. S. Qiang, L. G. Wei, P. Wang, H. J. Zhang, Y. L. Yang and Y. L. Wang, *J. Mater. Chem. A*, 2015, **3**, 6053; (e) L. Zhang, L. Rong, G. Hu, S. Jin, W.-G. Jia, J. Liu and G. Yuan, *Dalton Trans.*, 2015, **44**, 6731.
- 4 L.-L. Qu, Y.-L. Zhu, J. Zhang, Y.-Z. Li, H.-B. Du and X.-Z. You, *Crystengcomm*, 2012, **14**, 824; (b) H. Guo, Y. Yan, N. Wang, X. Guo, G. Zheng and Y. Qi, *Crystengcomm*, 2015, **17**, 6512; (c) X.-M. Wang, S. Chen, R.-Q. Fan, F.-Q. Zhang and Y.-L. Yang, *Dalton Trans.*, 2015, **44**, 8107.
- 5 (a) H. Shahroosvand, L. Najafi, E. Mohajerani, A. Khabbazi and M. Nasrollahzadeh, *J. Mater. Chem. C*, 2013, **1**, 1337; (b) V. Karunakaran, D. D. Prabhu and S. Das, *J. Phys. Chem. C*, 2013, **117**, 9404; (c) F. Monti, A. Baschieri, I. Gualandi, J. J. Serrano-Perez, J. M. Junquera-Hernandez, D. Tonelli, A. Mazzanti, S. Muzzioli, S. Stagni, C. Roldan-Carmona, A. Pertegas, H. J. Bolink, E. Orti, L. Sambri and N. Armaroli, *Inorg. Chem.*, 2014, **53**, 7709; (d) M. V. Werrett, G. S. Huff, S. Muzzioli, V. Fiorini, S. Zacchini, B. W. Skelton, A. Maggiore, J. M. Malicka, M. Cocchi, K. C. Gordon, S. Stagni and M. Massi, *Dalton Trans.*, 2015, **44**, 8379; (e) Z.-y. Shi, Z.-y. Zhang, J. Peng, X. Yu and X. Wang, *Crystengcomm*, 2013, **15**, 7199.
- 6 (a) X.-Y. Lv, M.-S. Wang, C. Yang, G.-E. Wang, S.-H. Wang, R.-G. Lin and G.-C. Guo, *Inorg. Chem.*, 2012, **51**, 4015; (b) R.-G. Lin, G. Xu, M.-S. Wang, G. Lu, P.-X. Li and G.-C. Guo, *Inorg. Chem.*, 2013, **52**, 1199; (c) C.-J. Zhang, Z.-W. Chen, R.-G. Lin, M.-J. Zhang, P.-X. Li, M.-S. Wang and G.-C. Guo, *Inorg. Chem.*, 2014, **53**, 847; (d) Z.-W. Chen, G. Lu, P.-X. Li, R.-G. Lin, L.-Z. Cai, M.-S. Wang and G.-C. Guo, *Cryst. Growth Des.*, 2014, **14**, 2527; (e) P.-X. Li, M.-S. Wang, L.-Z. Cai, G.-E. Wang and G.-C. Guo, *J. Mater. Chem. C*, 2015, **3**, 253.
- 7 (a) Y. Feng, X. Liu, L. Duan, Q. Yang, Q. Wei, G. Xie, S. Chen, X. Yang and S. Gao, *Dalton Trans.*, 2015, **44**, 2333; (b) E. S. Andreiadis, R. Demadrille, D. Imbert, J. Pecaut and M. Mazzanti, *Chem.-Eur. J.* 2009, **15**, 9458; (c) B. Liu, L. Bai, X. Lin, K. Li, H. Huang, H. Hu, Y. Liu and Z. Kang, *Crystengcomm*, 2015, **17**, 1686; (d) Y.-H. Tan, J.-X. Gao, Z.-F. Gu, Q. Xu, C.-S. Yang, Y.-S. Luo, B. Wang, Y.-Z. Tang and H.-R. Wen, *Polyhedron*, 2015, **101**, 239; (e) H. Shahroosvand, L. Najafi, E. Mohajerani, M. Janghour, M. Nasrollahzadeh, *RSC Adv.*, 2013, **3**, 6323.
- 8 (a) S.-H. Wang, F.-K. Zheng, M.-J. Zhang, Z.-F. Liu, J. Chen, Y. Xiao, A.-Q. Wu, G.-C. Guo and J.-S. Huang, *Inorg. Chem.*, 2013, **52**, 10096; (b) Y. Xiao, S.-H. Wang, F.-K. Zheng, M.-F. Wu, J. Xu, Z.-F. Liu, J. Chen, R. Li and G.-C. Guo, *Crystengcomm*, 2016, **18**, 721.
- 9 *CrystalClear, version 1.35; Software User's Guide for the Rigaku R-Axis, and Mercury and Jupiter CCD Automated X-ray Imaging System*, Rigaku Molecular Structure Corporation, Utah, 2002.
- 10 *SHELXTL Reference Manual, version 5*, Siemens Energy & Automation Inc., Madison, WI, 1994.
- 11 Gaussian 09, Revision D.01, M. J. Frisch, G. W. Trucks, H. B. Schlegel, G. E. Scuseria, M. A. Robb, J. R. Cheeseman, G. Scalmani, V. Barone, B. Mennucci, G. A. Petersson, H. Nakatsuji, M. Caricato, X. Li, H. P. Hratchian, A. F. Izmaylov, J. Bloino, G. Zheng, J. L. Sonnenberg, M. Hada, M. Ehara, K. Toyota, R. Fukuda, J. Hasegawa, M. Ishida, T. Nakajima, Y. Honda, O. Kitao, H. Nakai, T. Vreven, J. A. Montgomery, Jr., J. E. Peralta, F. Ogliaro, M. Bearpark, J. J. Heyd, E. Brothers, K. N. Kudin, V. N. Staroverov, T. Keith, R. Kobayashi, J. Normand, K. Raghavachari, A. Rendell, J. C. Burant, S. S. Iyengar, J. Tomasi, M. Cossi, N. Rega, J. M. Millam, M. Klene, J. E. Knox, J. B. Cross, V. Bakken, C. Adamo, J. Jaramillo, R. Gomperts, R. E. Stratmann, O. Yazyev, A. J. Austin, R. Cammi, C. Pomelli, J. W. Ochterski, R. L. Martin, K. Morokuma, V. G. Zakrzewski, G. A. Voth, P. Salvador, J. J. Dannenberg, S. Dapprich, A. D. Daniels, O. Farkas, J. B. Foresman, J. V. Ortiz, J. Cioslowski, and D. J. Fox, Gaussian, Inc., Wallingford CT, 2013.
- 12 M.-F. Wu, Z.-F. Liu, S.-H. Wang, J. Chen, G. Xu, F.-K. Zheng, G.-C. Guo and J.-S. Huang, *CrystEngComm*, 2011, **13**, 6386.
- 13 C. Janiak, *J. Chem. Soc., Dalton Trans.*, 2000, 3885.
- 14 (a) S.-H. Wang, F.-K. Zheng, M.-F. Wu, Z.-F. Liu, J. Chen, G.-C. Guo and A. Q. Wu, *Crystengcomm*, 2013, **15**, 2616; (b) M.-F. Wu, T.-T. Shen, S. He, K.-Q. Wu, S.-H. Wang, Z.-F. Liu, F.-K. Zheng and G.-C. Guo, *Crystengcomm*, 2015, **17**, 7473.
- 15 V. W. W. Yam and K. K. W. Lo, *Chem. Soc. Rev.*, 1999, **28**, 323.
- 16 (a) C. A. Bauer, T. V. Timofeeva, T. B. Settersten, B. D. Patterson, V. H. Liu, B. A. Simmons and M. D. Allendorf, *J. Am. Chem. Soc.*, 2007, **129**, 7136; (b) F. P. Doty, C. A. Bauer, A. J. Skulan, P. G. Grant and M. D. Allendorf, *Adv. Mater.*, 2009, **21**, 95.
- 17 (a) Z. F. Chen, R. G. Xiong, J. Zhang, X. T. Chen, Z. L. Xue and X. Z. You, *Inorg. Chem.*, 2001, **40**, 4075-4077; (b) D. P. Martin, M. A. Braverman and R. L. LaDuca, *Cryst. Growth Des.*, 2007, **7**, 2609.
- 18 T. M. Bockman and J. K. Kochi, *J. Org. Chem.*, 1990, **55**, 4127.
- 19 (a) W.-W. Zhou, J.-T. Chen, G. Xu, M.-S. Wang, J.-P. Zou, X.-F. Long, G.-J. Wang, G.-C. Guo and J.-S. Huang, *Chem. Commun.*, 2008, **24**, 2762; (b) P.-X. Li, M.-S. Wang, M.-J. Zhang, C.-S. Lin, L.-Z. Cai, S.-P. Guo and G.-C. Guo, *Angew. Chem. Int. Ed.*, 2014, **53**, 11529.

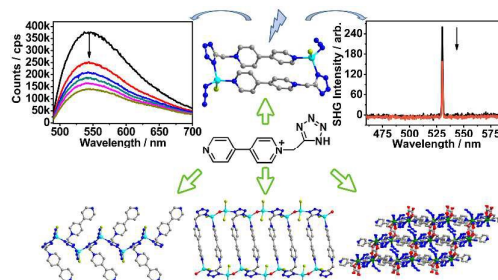
## Graphical Abstract

### Fluorescent and photochromic properties of a series of new Zn(II)/Cd(II) coordination compounds with a flexible semi-rigid tetrazole-viologen derivative

Yu Xiao,<sup>ab</sup> Shuai-Hua Wang,<sup>\*a</sup> Ya-Ping Zhao,<sup>ab</sup> Fa-Kun Zheng,<sup>\*a</sup> and Guo-Cong Guo<sup>a</sup>

<sup>a</sup> State Key Laboratory of Structural Chemistry, Fujian Institute of Research on the Structure of Matter, Chinese Academy of Sciences, Fuzhou, Fujian 350002, P. R. China

<sup>b</sup> University of Chinese Academy of Sciences, Beijing 100039, P. R. China



The diverse luminescence was realized by rational design and construction of a series of Zn(II)/Cd(II) coordination compounds. Especially, the isolated binuclear compound shows interesting photochromic characteristic, and exhibits fluorescence and second-order nonlinear optical properties variation upon ultraviolet light irradiation.